Microelectronic Engineering 87 (2010) 2633–2637

Contents lists available at ScienceDirect

Microelectronic Engineering

journal homepage: www.elsevier.com/locate/mee

Polishing behaviors of single crystalline ceria abrasives on silicon dioxide and silicon nitride CMP

Myoung-Hwan Oh [a,*], Rajiv K. Singh [a], Sushant Gupta [a], Seung-Beom Cho [b]

[a] Department of Materials Science and Engineering, University of Florida, Gainesville, FL 32611, USA
[b] LG Chem. Ltd./Research Park, I&E materials, 104-1 Moonji-dong, Yuseong-gu, Daejeon 305-380, Republic of Korea

ARTICLE INFO

Article history:
Received 13 May 2010
Accepted 28 July 2010
Available online 4 August 2010

Keywords:
Ceria
Abrasive
Chemical mechanical polishing (CMP)
Removal selectivity

ABSTRACT

The effects of single crystalline ceria (CeO_2) abrasives in chemical mechanical polishing (CMP) slurries were investigated for silicon dioxide (SiO_2) and silicon nitride (Si_3N_4) CMP process. The size of ceria abrasives was controlled by varying hydrothermal reaction conditions. Polishing removal rate was measured with four slurries, with different mean primary particle size of 62, 116, 163 and 232 nm. The polishing results showed that the single crystalline ceria abrasives were not easily broken-down by mechanical force during CMP process. It was found that the removal rate of oxide and nitride film strongly depend upon abrasive size, whereas the surface uniformity deteriorates as abrasive size increases. The observed polishing results confirmed that there exists an optimum abrasive size (163 nm) for maximum removal selectivity between oxide and nitride films. The polishing behavior of the single crystalline ceria abrasives was discussed in terms of morphological properties of the abrasive particle.

1. Introduction

Ceria particles have been widely used as abrasives for glass polishing and CMP of oxide films due to the high removal rates for oxide films and the softness of the particles [1,2]. Ceria-based slurry has been used in CMP of shallow trench isolation (STI) structures consisting of silicon dioxide and silicon nitride layers due to its high selectivity over nitride layer [3,4]. For the STI-CMP process, high removal selectivity is very important for reduction of the CMP defects and endpoint detection. During the past decade, mechanical properties, chemical aspects and morphological characteristics of the ceria abrasives have been identified as important parameters that influence the STI-CMP performance [5,6]. Therefore, many approaches to control these properties of ceria abrasives have been extensively investigated.

The usual method for synthesizing ceria abrasives is thermal decomposition of the cerium salt such as cerium carbonate and cerium hydroxide [7,8]. These ceria abrasives have polycrystalline structure with an easily brittle system, which affects a high removal rate of oxide films during polishing. However, the size and the shape of ceria abrasives are very limited since particle growth is difficult to control during calcination process. The irregular shape and aggregates lead to defects on the surface of film during CMP process. To achieve the desired particle size and the uniform particle size distribution, thermal technique requires a complicated combination of mechanical milling process and filteration system [9]. Other methods for preparing ceria abrasives are liquid phase processes [10,11]. These methods can lead to ceria abrasives with controllable size by manipulating reaction parameters. However, the size of ceria abrasives is limited to less than 50 nm leading to a low removal rate during CMP process.

To overcome these problems, hydrothermal method is proposed to synthesize the ceria abrasives with a well-defined morphology. Hydrothermal synthesis is a very efficient method for controlling the morphological properties and crystalline size of the solid particles without calcination and mechanical milling process [12]. In addition, the ceria particles obtained by this method have several advantages over other methods such as narrow size distribution, desirable characteristics including very fine size, high chemical purity and good chemical homogeneity [11]. However, this method has seldom been applied to the synthesis of ceria abrasives for CMP slurry. Furthermore, previous studies for the polishing performance of ceria abrasives have limited to polishing behaviors of polycrystalline ceria particles and silica layer and have mainly focused on the chemical interactions between ceria abrasives and silica layer during CMP process.

In this work we synthesized the single crystalline ceria particles of different mean sizes using hydrothermal method. For CMP performance evaluation, the effect of single crystalline ceria abrasives on the removal rate, the oxide–nitride removal selectivity and within-wafer nonuniformity (WIWNU) was investigated.

* Corresponding author. Tel.: +1 352 846 2496; fax: +1 352 392 3771.
E-mail address: mhplusmy@ufl.edu (M.-H. Oh).

0167-9317/$ - see front matter © 2010 Elsevier B.V. All rights reserved.
doi:10.1016/j.mee.2010.07.040

2. Experimental

2.1. Preparation of ceria abrasives by hydrothermal method

Cerium (III) nitrate hexahydrate ($Ce(NO_3)_3{\cdot}6H_2O$) and potassium hydroxide (KOH) were used as the starting materials for the ceria precursor. Cerium (III) nitrate hexahydrate (0.5 M) and of potassium hydroxide 0.5 M were separately dissolved in mixed solvent of deionized (DI) water and ethylene glycol ($C_2H_6O_2$). The volume ratio of ethylene glycol to water was kept at 2:3. The reaction was carried out at a temperature of 50 °C with stirring rate of 100 rpm for 12 h. Air was bubbled into the precipitation reactor with passage through a gas distributor as an oxidizer. The precipitated ceria precursor was separated via centrifugation and then redispersed in distilled water under continuous stirring. The weight ratio of distilled water to the precipitated ceria precursor was kept constant at 5:1. The pH of the suspension solution was adjusted between pH 0.5 and 3.0 by adding concentrated nitric acid (HNO_3). The sol-type ceria precursor was kept in an autoclave with a reaction chamber of 2 L. Three quarters of the volume of the chamber was filled with the ceria precursor. The hydrothermal reaction was carried out at 220–230 °C for 6 h. After the hydrothermal reaction, the synthesized particles were washed with distilled water three times. The crystal structure and grain size was identified by X-ray diffraction (XRD) using CuKα radiation. The grain size was estimated by the Scherrer equation according to the formula $D = 0.9\lambda/(\beta\cos\theta)$, where D is the grain size, λ is the wavelength of X-rays, β is the half-width of the diffraction peaks, and θ is the diffraction angle. The broadening of the reflection from the (1 1 1) plane was used to calculate the grain size. The morphology and size of the precipitate particles were examined by high resolution transmission electron microscope (HRTEM) and field emission scanning electron microscope (FESEM). The average primary particle size was calculated by measuring ca. 100 particles from FESEM micrographs. The specific surface area (SSA) of the ceria abrasives was determined by Brunauer–Emmett–Teller (BET) method using nitrogen adsorption/desorption at 77 K.

2.2. Polishing of the wafers

Different ceria-based slurries were formulated by dispersing abrasives each with different primary particle size in DI water containing an anionic organic polymer (Poly acrylic acid, PAA, Mw 4000, LG Chem.) as dispersant. 2 wt.% of PAA based on the total weight of the ceria abrasives was added. For each slurry, pH was adjusted to 6.5–6.7 by adding ammonium hydroxide (NH_4OH). The solid loading of ceria abrasives was fixed to 2.0 wt.%. Table 1 presents the slurry characteristics used in polishing tests. The abrasive size distribution of slurry was measured using light scattering method (UPA 150, Microtrac Inc.).

Silicon dioxide film of 2 μm thick was grown on a 4-in. p-type silicon substrates with (0 0 1) orientation by plasma enhanced chemical vapor deposition (PECVD). The silicon nitride films were deposited by using low-pressure chemical vapor deposition (LPCVD). Polishing tests were performed on a rotary type CMP machine (GNP POLI 400, G&P technology) for 1 min with each of the ceria-based slurries. IC 1000/SUBA IV stacked pads (supplied by Rodel Inc.) were utilized as CMP pads. The downforce was 280 g/cm^2 and the rotation speed between the pad and the wafer was 90 rpm. The slurry flow rate was 100 mL/min. The film thickness on the wafers before and after CMP was measured using spectroscopic reflectometry (Nanospec 6100, Nanometrics) to calculate the removal rate. In this experiment, the WIWNU was defined as the standard deviation of remaining thickness divided by the average of the remaining thickness after the CMP process. The average polishing data for removal rate was carried by performing the same tests more than three times in order to support the validity of the results from the statistical viewpoint.

3. Results and discussion

3.1. Ceria abrasives

Fig. 1 shows the four types of abrasive particles prepared in different hydrothermal conditions as described in Table 1. The primary particle sizes determined in the FESEM examination were 62, 116, 163 and 232 nm for slurry A, B, C and D, respectively. The well-dispersed particles of spherical shape as shown in Fig. 1(a) were transformed into square shape as a result of grain growth which is clearly seen from FESEM image (Fig. 1(d)). These images indicate that the primary particle size increases with hydrothermal temperature and strength of acidic medium and the morphology of abrasives can be controlled by changing the hydrothermal conditions, which affect the grain growth of ceria crystallites.

The major reflections associated with cubic fluorite structure of ceria can be observed from the XRD pattern as shown in Fig. 2. Sharp intensity peaks are observed for ceria abrasives with increased primary particle size. The average grain size of various abrasives was calculated from the Scherrer equation by using the line-broadening of the (1 1 1) peak in XRD pattern. The grain size gradually increased from 29 to 66 nm as the hydrothermal temperature and the acidity of hydrothermal medium were increased. This result coincides with the trend of increasing primary particle size in the FESEM images shown in Fig. 1.

Fig. 3 shows the high resolution TEM images of two samples with average particle diameters of 62 nm and 232 nm, respectively. As shown in Fig. 3(a), the sample with diameter of 62 nm appears to be well-defined crystallites based on the fact that the lattice fringes corresponding to the (1 1 1) reflections are clearly observed from the crystal orientation. For 232 nm ceria particle, the TEM image (Fig. 3(b)) shows homogenous single phase of the lattice fringes without disorder and defects in the lattice. These results indicate that ceria abrasives used in this study have a single crystalline structure regardless of grain growth and particle size.

3.2. Characteristics of ceria abrasive before and after CMP

To evaluate the effects of single crystalline ceria abrasives, polishing tests for four types of slurries with different abrasive parti-

Table 1
Comparison of slurries used in this study.

Samples	Hydrothermal conditions		Primary particle size (SEM, nm)	Grain size (XRD, nm)	Slurry mean size (UPA, nm)	Surface area (m^2/g)
	pH	Temp. (°C)				
Slurry A	3.0	220	62	29	178	22.12
Slurry B	3.0	230	116	40	273	16.37
Slurry C	1.5	230	163	45	326	11.44
Slurry D	0.5	230	232	66	484	7.48

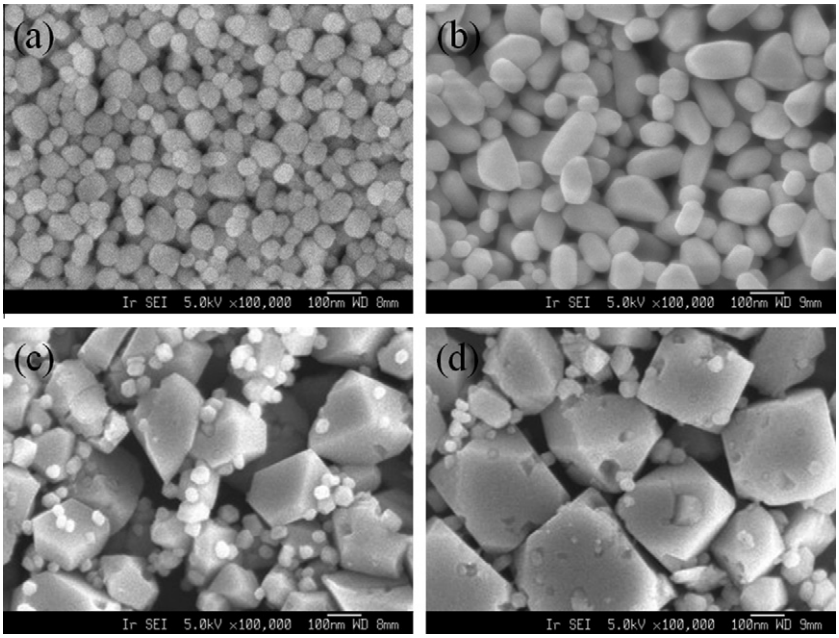

Fig. 1. FESEM photographs of the ceria particles prepared with different hydrothermal conditions; (a) pH 3.0 at 220 °C, (b) pH 3.0, (c) pH 1.5 and (d) pH 0.5 at 230 °C, respectively.

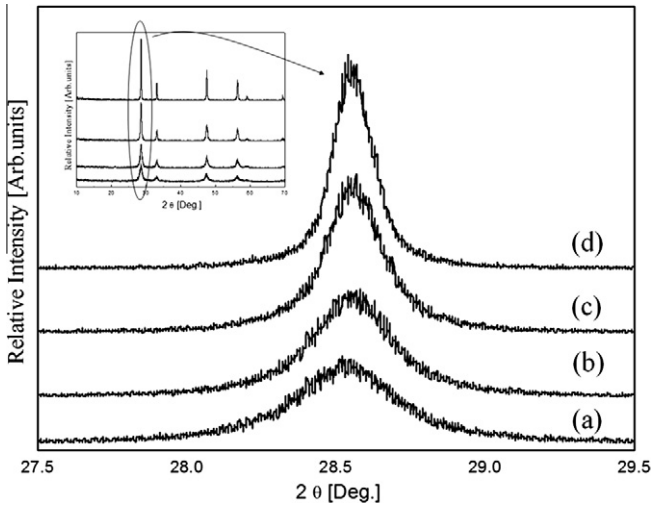

Fig. 2. XRD patterns and the (1 1 1) peaks analyzed to confirm grain size of the ceria abrasives dispersed in ceria-based slurry (a) A, (b) B, (c) C and (d) D.

cle size were preformed. Fig. 4 shows the particle size distribution of different slurries without PAA dispersant. The size distribution of secondary particle size determined by light scattering method were 178, 273, 326 and 484 nm for slurry A, B, C and D, respectively. The dispersed particle size is much larger than the crystallite size estimated by X-rays and the primary particle size calculated by FESEM. This mismatch in size is due to extensive overlapping of the ceria particles in water-based solution [13]. As shown in Fig. 4, the increase in size of the primary particles led to broader particle size distribution in water-based solution. Fig. 5 shows the FESEM images of ceria abrasives before and after silicon dioxide polishing for slurry D. The ceria abrasives after polishing were washed with distilled water three times via centrifugation. According to Fig. 5, no definitive difference between both abrasives before and after polishing can be seen except that square edges of some abrasives were changed to round edges after polishing. This indicates that the single crystalline ceria abrasives synthesized in this study are less brittle and do not fracture upon applied pressure during polishing.

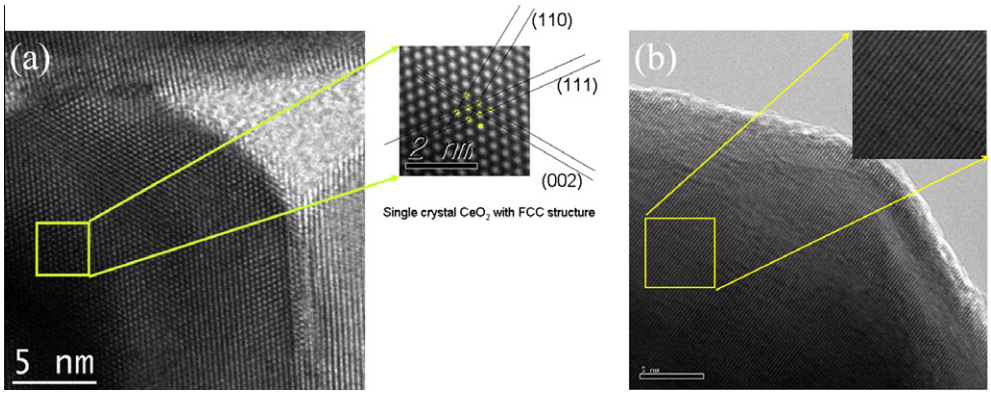

Fig. 3. FETEM micrographs and of ceria abrasive with average particle diameters of (a) 62 nm (slurry A) and (b) 232 nm (slurry D).

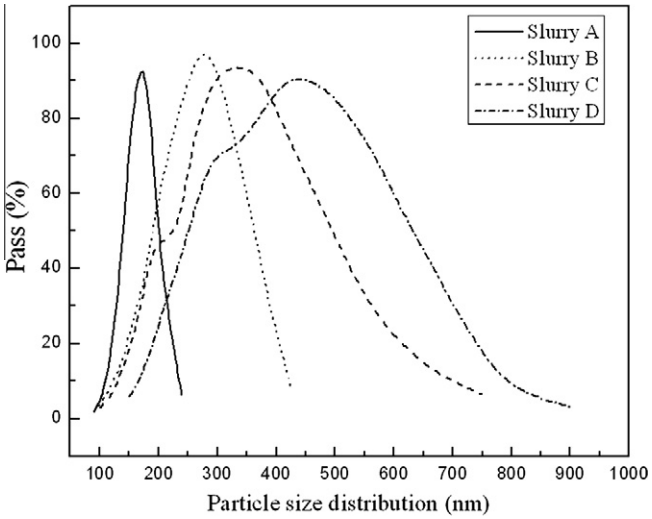

Fig. 4. Particle size distribution of ceria-based slurry used in this study.

3.3. Polishing performance

Fig. 6 shows the results of CMP field evaluation and quantitative results of the slurry are presented in Table 2. For oxide CMP process, it is clear that the removal rate increases with increasing size of ceria abrasives. The polishing of oxide film is mainly affected by the chemical contribution of ceria particles and mechanical factors, such as the CMP conditions, morphological characteristics of abrasives and particles size distribution. During the polishing of the oxide film, ceria abrasives exhibit a chemical tooth property [1]. As a consequence, chemical interaction between the silica film and the ceria abrasives occur during CMP process and Si–O–Ce bonding is formed on the surface of silica film. The Si–O–Ce bonds can be rapidly removed by the mechanical force generated by pressed pad. This physicochemical reaction leads to the high removal rates of oxide film. Furthermore, polishing behavior is closely associated with shape and size of the ceria abrasives. As shown in Fig. 1, the shape of the small abrasives (Fig. 1(a) and (b)) is spherical, whereas the large abrasives (Fig. 1(a) and (b)) have a square shape with sharp edges. The sharp edge and large size of abrasive particles can induce higher local pressure to generate more frictional force during polishing.

The removal rate of nitride film increases with the increase in the abrasive size. According to previous report [8], the removal rate of nitride film is affected by the physical properties of ceria-based slurry systems and the amount of surfactant adsorbed on the film surface. In order to improve the selectivity and uniformity, an anionic acrylic polymer is generally used to passivate the surface of the nitride film during STI-CMP, which prevents ceria abrasives from contacting the film surface [14]. In this study, the amount of polymer added was same for all the slurries. Therefore, it seems that the increase in removal rate of the nitride film is related to the mechanical factors rather to the effect of adsorbed polymer passivation layer. These mechanical factors are influenced by several physical parameters of the CMP process, such as morphological aspects of the abrasives, crystallite size of the abrasives and the CMP conditions.

The removal selectivity can be calculated by comparing the removal rate between oxide and nitride film. As shown in Fig. 6(a), the removal selectivity showed a transition behavior at the slurry

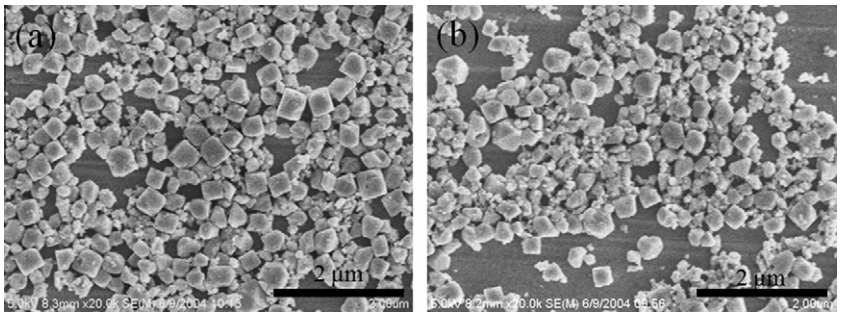

Fig. 5. FESEM photographs of ceria abrasives (a) before and (b) after oxide CMP process.

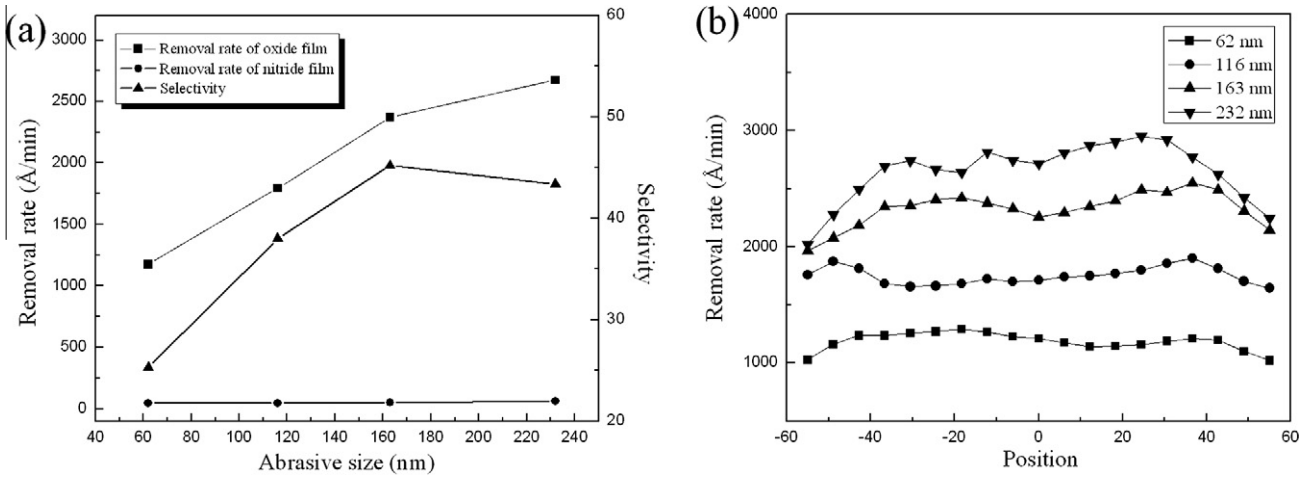

Fig. 6. Results of CMP field evaluation: (a) removal rate and selectivity and (b) within-wafer nonuniformity (WIWNU) of silica film.

Table 2
The results of the CMP evaluation.

Samples	Oxide removal rate (Å/min)	Nitride removal rate (Å/min)	Selectivity	WIWNU of oxide film (%)
Slurry A	1174.4 ± 105.1	46.4 ± 3.3	25.3 ± 0.5	3.0
Slurry B	1794.2 ± 125.5	47.3 ± 3.7	38.0 ± 0.6	5.5
Slurry C	2369.4 ± 194.3	52.4 ± 4.3	45.2 ± 0.1	8.1
Slurry D	2674.1 ± 201.8	61.6 ± 5.3	43.4 ± 0.5	11.89

C. The removal rate of oxide film rapidly increased from 1174 Å/min at 62 nm to 2369 Å/min at 163 nm, whereas it slowly increased to 2674 Å/min for 232 nm. This phenomenon is explained by two related factors: the contact area reduction [15] and the particle surface activity [8]. In the case of oxide CMP process, the polishing behavior should be also considered from the viewpoint of the contact area between the abrasives and the film surface. According to contact area mechanism [16,17], the removal rate increases with decreasing abrasive size and increasing solid loading, due to the increase in contact area between the abrasives and the film surface. At a fixed solid loading, the number of ceria abrasives in slurry decrease as the abrasive size increases which leads to relatively low removal rate for the target material during CMP process even though the abrasive size increases. For nitride film, the removal rate increased slightly and did not vary much with increasing abrasive size, which can be explained by the relationship between additive polymer and abrasive size. The additive polymer can be more easily attached on the surface of the small abrasives than on the surface of large ones, due to high surface activity and specific surface area of the small abrasives. The slurry with small abrasives can induce a relatively high removal rate for nitride film in comparison with its abrasive size, since the passivation layer is insufficiently formed on the nitride film surface as polymer is largely adsorbed on the particle surface. As described in Table 1, the specific surface area decreased with increasing abrasive size. This means that removal rate for nitride film can be relatively increased in spite of decrease in the abrasive size. As a result, the removal rate of nitride film showed relatively low increase in rates with increase in the abrasive size. Such behavior is suggestive of existence of an optimum size of ceria abrasives for high removal selectivity.

Additionally, the results for surface uniformity of the oxide films are shown in Fig. 6(b). The slurry shows a higher WIWNU for the oxide film with increase in the size of ceria abrasives. This polishing behavior is attributed to a broader particle size distribution of the slurry and the shape of the large abrasives. The distribution data in Fig. 4 shows that the particle size distribution broadens with the increase in abrasive size. The broader particle size distribution of large abrasives can cause different removal rates between the center and the edge of the wafer due to their limited mobility on the wafer surface. This result is also consistent with the observations of Moudgil et al. [17]. They investigated the polishing mechanism of slurry with non-uniform particle size distribution, which not only created surface deformation but also changed the polishing removal rate. In this report, the sharp edge of the abrasives can be regarded as another factor for roughness of wafer. The film abraded by the sharp edge has a higher local pressure to generate more friction force during polishing. This can induce a significant increase in the local surface roughness caused by pit formation on the wafer surface [18]. As a result, the surface uniformity shows deterioration with increase in abrasive size. Therefore, it seems that surface uniformity of oxide film is related to the mechanical factors and morphological properties of ceria abrasives and particle uniformity of the ceria-based slurry. Interestingly, there exists an optimum abrasive size distribution at which enhanced removal rates and selectivity are observed.

4. Conclusions

In this study, we investigated the effects of single crystalline ceria abrasives on polishing performance during silicon dioxide and silicon nitride CMP. The abrasive size was directly controlled by varying hydrothermal conditions without post-heat treatment and mechanical milling process. The results showed that the single crystalline ceria abrasives were not easily broken-down by mechanical force between abrasives and film surface during polishing. With increasing abrasive size, the removal rate of silicon dioxide and silicon nitride films increased. On the other hand, the surface uniformity deteriorated with increasing abrasive size, due to a broader particle size distribution of the abrasives in slurry and the morphology of the large abrasives. In addition, the removal selectivity showed a transition at the slurry C (with particle size of 163 nm). Considering these polishing behaviors of single crystalline ceria abrasives, it was found that there exists an optimum abrasive size for optimum removal rate and selectivity in silicon dioxide and silicon nitride CMP.

References

[1] L.M. Cook, J. Non-Cryst. Solids 120 (1990) 152–171.
[2] G.V. Samsonov, The Oxide Handbook, second ed., IPI/Plenum Data, New York, 1982.
[3] P.W. Carter, T.P. Johns, Electrochem. Solid-state Lett. 8 (8) (2005) G218–G221.
[4] D.S. Lim, J.W. Ahn, H.S. Park, J.H. Shin, Surf. Coat. Technol. 200 (2005) 1751–1754.
[5] S.K. Kim, S. Lee, U. Paik, T. Katoh, J.G. Park, J. Mater. Res. 18 (9) (2003) 2163–2169.
[6] P. Janos, M. Petrak, J. Mater. Sci. 26 (1991) 4062–4066.
[7] E. Matjevic, W. Hsu, J. Colloid Interface Sci. 118 (2) (1987) 506–523.
[8] Y.H. Kim, S.K. Kim, N.S. Kim, J.G. Park, U. Paik, Ultramicroscopy 108 (2008) 1292–1296.
[9] H.G. Kang, H.S. Park, U. Paik, J.G. Park, J. Mater. Res. 22 (3) (2007) 777–787.
[10] S.H. Lee, Z.L. Lu, S.V. Babu, E. Matijevic, J. Mater. Res. 17 (10) (2002) 2744–2749.
[11] N.C. Wu, E.W. Shi, Y.Q. Zheng, W.J. Li, J. Am. Ceram. Soc. 85 (10) (2002) 2462–2468.
[12] M. Hirano, Y. Fukuda, H. Iwata, Y. Hotta, M. Inagaki, J. Am. Ceram. Soc. 83 (5) (2000) 1287–1289.
[13] T. Allen, fifth ed., Particle Size Measurement, vol. 1, Chapman and Hall, New York, 1997.
[14] W.G. America, S.V. Babu, Electrochem. Solid-state Lett. 7 (12) (2004) G327–G330.
[15] M. Bielmann, Masters Thesis, University of Florida, Gainesville, FL, 1998.
[16] U. Mahajan, M. Bielmann, R.K. Singh, Mater. Res. Soc. Symp. Proc. 566 (1999) 27–31.
[17] G.B. Basim, J.J. Adler, U. Mahajan, R.K. Singh, M. Moudgil, J. Electrochem. Soc. 147 (2000) 3523–3528.
[18] T. Izumitani, in: M. Tomozawa, R. Doremus (Eds.), Treatise on Materials Science and Technology, Academic Press, New York, 1979, pp. 116–149.